The Anatomy of Radioisotope Lung Scanning

Nicholas W. Morrell, C. Michael Roberts, Barbara E. Jones, Kuldip S. Nijran, Tony Biggs, and W. Anthony Seed

Departments of Medicine and Nuclear Medicine, Charing Cross and Westminister Medical School, London, United Kingdom

An appreciation of the appearances of segmental and lobar defects on a lung scan is important for the diagnosis of pulmonary embolism. The appearances of segmental and lobar ventilation defects of known anatomical location have been examined on ^{81m}Kr ventilation scans in normal human subjects, utilizing fibreoptic bronchoscopy to place temporary occlusions under direct vision at the orifices of lobar and segmental bronchi. Scans were obtained in the posterior, posterior-oblique and lateral projections. Anterior views were included if the defects could not be adequately visualized on the other views. The completeness of the occlusion and the site and size of each defect could be confirmed by ventilating the segment itself with ^{81m}Kr via the balloon catheter while the occlusion was maintained. Segmental defects located anterior to the hilum of the lung tended to be optimally visualized on the lateral view and defects located posterior to the hilum tended to be optimally visualized on the posterior-oblique view. The size of segmental defects could be underestimated on the lung scan, especially those involving the anterior and lateral basal segments of both lower lobes. Defects involving the medial basal segment of the right lower lobe were undetectable on any view. By implication, the same conclusions apply to ^{99m}Tc perfusion scans.

J Nucl Med 1992; 33:676–683

In studies of the value of ventilation-perfusion lung scanning for the diagnosis of pulmonary embolism, it is widely held that the identification of segmental and larger perfusion defects, not matched by ventilation, carries a higher probability for pulmonary embolism than subsegmental defects or defects not corresponding to known anatomical boundaries (*1–6*). More recently this has been confirmed prospectively (*7,8*).

Thus, mismatched ventilation-perfusion scans have been classified into those having a low, intermediate or high probability for pulmonary embolism depending on the size, number and location of defects. For example, in the recent Prospective Investigation of Pulmonary Embolism Diagnosis (PIOPED) study (*8*), nonsegmental and small defects (<25% of a bronchopulmonary segment) were assigned a low probability, as were single moderate defects (>25% but <75% of a segment). On the other hand, the presence of two or more large defects (>75% of a segment) was judged to have a high probability for pulmonary embolism.

Despite the importance of segmental anatomy to these conclusions, little has been done to define the precise appearance of segmental defects on a lung scan. In general terms, a segmental defect has been described as a peripheral concave or triangular defect that is pleurally based and corresponds to known anatomical boundaries (*9*). A subsegmental defect has been described as a defect "within the distribution of an anatomic lung segment that is smaller in volume but clearly segmental in shape" (*10*). Atlases of segmental lung scan anatomy have been compiled using foam or plaster of Paris lung phantoms impregnated with radioisotopes (*11,12*) or by selecting scans from patients with a presumptive diagnosis of pulmonary embolism that most closely conform to the authors' interpretation of segmental anatomy (*13*). The aim of the present study is to demonstrate the appearances of known lobar and segmental defects on a lung scan in the human subject and to suggest optimal positioning for visualization of a defect. An appreciation of these appearances may help to increase the accuracy of ventilation-perfusion scanning in the diagnosis of pulmonary embolism.

METHODS

All subjects were healthy volunteers (n = 20) aged between 20 and 30 yr, with no history of chest disease and normal lung function. Each subject gave written informed consent and the project was approved by the local ethical committee. Subjects were premedicated with atropine and an opiate. Local anesthesia was achieved with nebulized lignocaine, supplemented if necessary with 2-ml aliquots of lignocaine via the bronchoscope. Subjects were also sedated with 2.5–5 mg of intravenous midazolam immediately prior to the procedure.

An Olympus BF-1T20D flexible fibreoptic bronchoscope, with a 5.9-mm external diameter and 2.8-mm diameter instrument channel was used throughout the study.

Subjects were positioned lying supine on a perspex table overlying a gamma camera with a low-energy, long-bore, parallel-hole collimator with the energy window settings at 20%. Ventilation scans were performed with ^{81m}Kr eluted from a ^{81}Rb generator by air delivered at 1.5 liters/min. This was inhaled by the subject during tidal respiration via a mouth piece and hose with one-way valves to allow for exhaust away from the gamma camera and to prevent rebreathing. Prior to bronchoscopy, control scans were

Received Oct. 18, 1991; revision accepted Dec. 13, 1991.

For reprints contact: Dr. Nicholas W. Morrell, Department of Medicine, Charing Cross Hospital, Fulham Palace Rd., London W6 8RF.

performed in the posterior, both posterior-oblique and lateral projections collecting 250K to 300K counts in each position.

The bronchoscope was then passed per-nasally to the central airways and a 6F balloon catheter (Cordis, USA; maximum inflation capacity 1.3 ml, giving a balloon diameter of 10 mm) was introduced via the instrument channel. Further control scans were then obtained to exclude any effect of the bronchoscope on the distribution of ventilation and identify any local ventilation defects caused by instillation of local anesthetic. The balloon was then inflated under direct vision at the orifice of a selected lobar or segmental bronchus and the bronchoscope withdrawn to the trachea.

Ventilation scans (Fig. 1)were performed in two ways: (1) with the subject breathing the air/^{81m}Kr mixture via the mouth to produce a "negative" image of the defect and (2) by ventilating the isolated segment with air/^{81m}Kr while the subject breathed room air. The air/^{81m}Kr was introduced with a hypodermic syringe via the lumen of the balloon catheter, which opens beyond the balloon occlusion. In this way "positive" scans of a segment were obtained.

Negative scans were performed in the posterior, posterior-oblique and lateral projections. Again 250K to 300K counts were collected in each view. Anterior views were included if the defect was not apparent on the other projections. Twenty-five thousand counts were collected to obtain the positive images.

Each study was limited by the duration of local anesthesia; two or sometimes three lobes or segments could be visualized in each study. A total of 25 bronchoscopies were performed. Five subjects were bronchoscoped twice. In some subjects supine and seated images were obtained to assess the effect of diaphragmatic position on the appearances of basal defects.

The absorbed radiation dose to the lung was calculated to be approximately 0.7 mSv per study (*14*).

RESULTS

Negative Images

The presence of the bronchoscope itself did not appear to produce defects in ventilation. However, injections of local anesthetic commonly caused defects in the region of the apical basal segment (the lowermost segment in the supine position). When these occurred, remote sites were chosen for occlusion studies.

Table 1 shows those views that best and worst demonstrated a known defect. Easily visualized segments were studied only once, the others at least twice. Occlusions of the medial basal segment of the right lower lobe, which were undetectable on any view, were attempted in two subjects. Figures 2–7 illustrate some of the results in Table 1.

Positive Images

Images produced by ventilating isolated segments with ^{81m}Kr were useful to confirm the anatomic location of the occlusion and to give an accurate indication of the surface projection of the segment involved. It also indicated whether leakage around the occlusion had occurred. It was not always possible to obtain technically acceptable positive images because:

1. The open tip of the catheter, distal to the balloon, often lay in a subsegmental bronchus.
2. Inflation of the balloon in a segmental bronchus would obstruct the orifices of subsegmental bronchi that branched early.

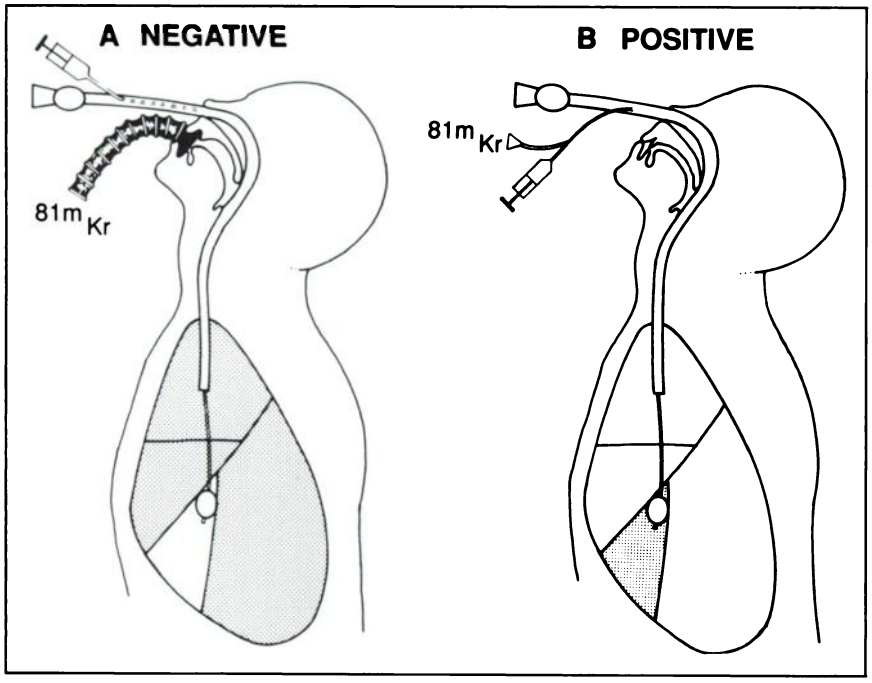

FIGURE 1. Two methods for imaging the lung with ^{81m}Kr. The catheter has been passed through the bronchoscope and the balloon inflated to obstruct a segmental bronchus. (A) Krypton-81m is inhaled via the mouthpiece to give a "negative" image. (B) Krypton-81m is injected through the catheter to give a "positive" image of the occluded lung segment beyond the balloon.

TABLE 1
Views Optimally Demonstrating a Segmental or Lobar Defect

	POST*	PO†	LAT‡
Left Upper Lobe			+
Apico-posterior		+	
Anterior	−		+
Lingula	−		+
Superior	−		+
Inferior	−		+
Left Lower Lobe		+	
Anterior	−		+
Apical		+	
Lateral	−	+	
Posterior		+	
Right Upper Lobe			+
Apical			+
Anterior		+	+
Posterior			
Right Middle Lobe			+
Medial		−	+
Lateral	−		+
Right Lower Lobe		+	
Medial	−	−	−
Anterior			+
Apical		+	
Lateral		+	
Posterior		+	

* Posterior; † posterior-oblique and ‡ lateral.

A + indicates the view optimally demonstrating a defect. A − indicates that a defect was not apparent in that view. A blank indicates that a defect was apparent but not optimally visualized.

Neither of these factors would affect the negative image but tended to make the positive image smaller, by excluding isotope from parts of the segment being studied. This was apparent by direct comparison of the positive and negative images.

When acceptable positive and negative images were obtained for a segment without the confounding factors just mentioned, there was a tendency for the negative image to underestimate the size of the defect. This was particularly noted in the anterior and lateral basal segments of both lower lobes (Fig. 8).

Seated Images

It proved difficult to obtain comparable images in the seated and supine positions because of coughing provoked by changing posture and because of difficulties in keeping a partially sedated subject still long enough to acquire the image. Limited images were obtained of the anterior and lateral basal segments. Defects were apparent in both positions but with little difference between them (Fig. 9).

DISCUSSION

This study was designed to define precisely the lung scan appearances of known segmental defects and to clarify which projections are diagnostically most useful in their detection. An isotope was used (^{81m}Kr) that gives similar resolution to ^{99m}Tc used in perfusion scanning (*15*). In the lung, the territory perfused by an artery supplying a bronchopulmonary segment is the same as that ventilated via its segmental bronchus (*16*). Therefore, the scan images of segmental defects in ventilation are directly comparable with corresponding segmental perfusion defects. For this reason the present observations are relevant to anatomical criteria used in the diagnosis of pulmonary embolism.

The scans were used to define the optimal projection in which to visualize individual segmental defects for diagnostic purposes. Images were obtained in the posterior, posterior-oblique and lateral projections and a view was considered optimal if it demonstrated the defect at its

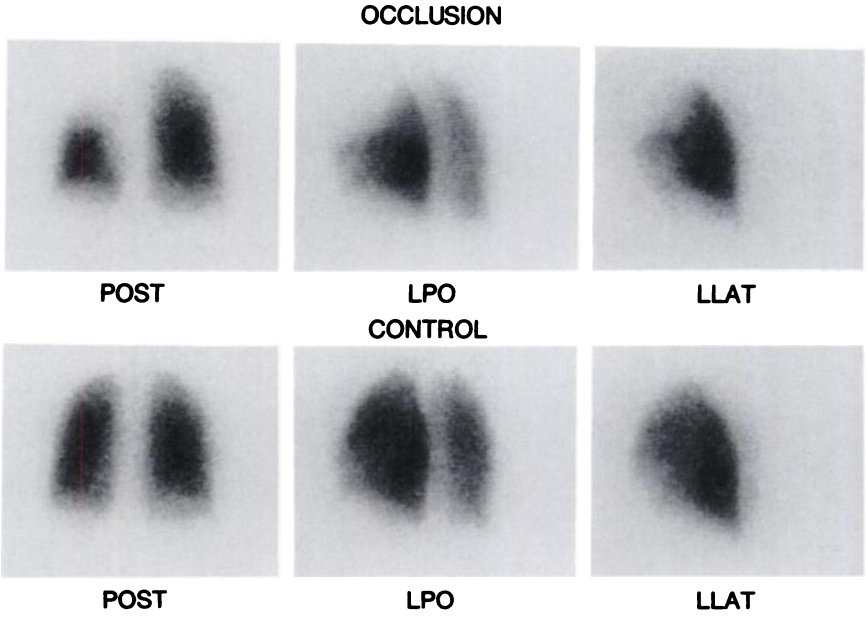

FIGURE 2. (Upper) Left upper lobe occlusion. (Lower) Control views (same subject). The defect is apparent in all views, but its lobar nature is only appreciated in posterior-oblique and lateral views where the lobar boundaries are seen in profile. (POST = posterior, LPO = left posterior oblique and LLAT = left lateral).

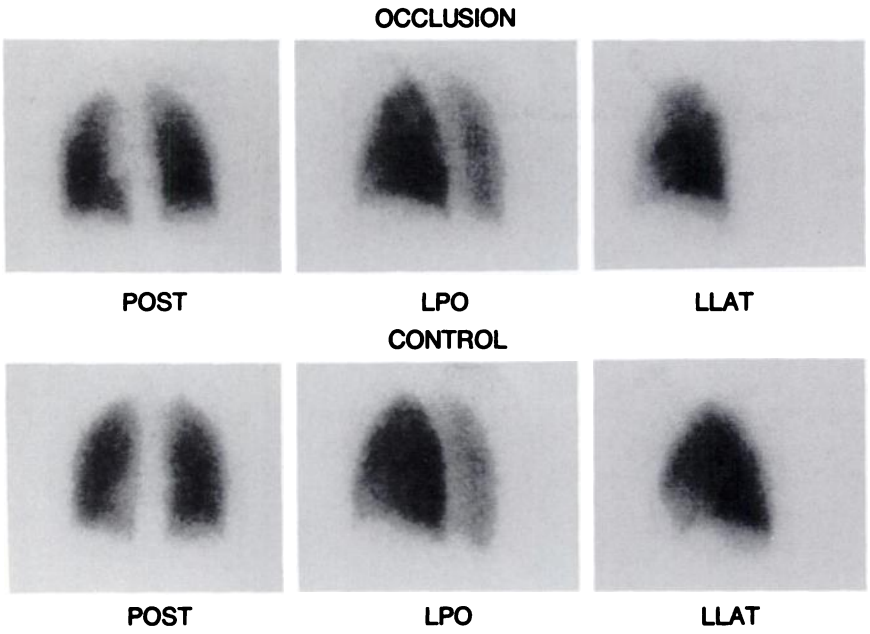

FIGURE 3. Defect involving the anterior segment of the left upper lobe. Same layout as for Figure 2. The defect is not apparent in the posterior view and it is only in the left lateral view that the segmental boundaries are clear.

largest with its boundaries clearly visible. The anterior view was examined if a defect was not clearly apparent in the other projections. Anterior-oblique views were not included in the present study. Nielsen et al. (*17*) found that they contributed little and did not demonstrate defects which were not already apparent on the other views.

The data in Table 1 indicate that the posterior view is never optimal. The posterior-oblique view proved the most useful view in 7 of 18 segments, while the lateral view provided optimal visualization of 9 of 18 segments studied. The posterior-oblique view has been considered to be the best view in previous clinical studies (*17,18*). One explanation for the disparity between this conclusion and the present study is that the previous studies looked at scan abnormalities in other conditions as well as pulmonary embolism. A further explanation is that in pulmonary embolism the lower lobes are more frequently involved (*19*) and it is the segmental defects in these lobes (with the exception of the anterior segment) that were better visualized by the posterior-oblique view in our study.

It has been claimed that "shine-through" of radioactivity from the other lung may adversely affect the resolution of defects in the lateral projection (*20*). However, Surprenant (*21*) found experimentally that this was not the case, but that shine-through from the same lung may more easily mask lesions in the anterior and posterior projections. Our findings support this: the more anteriorly placed segments are better visualized on the lateral scan, because in this

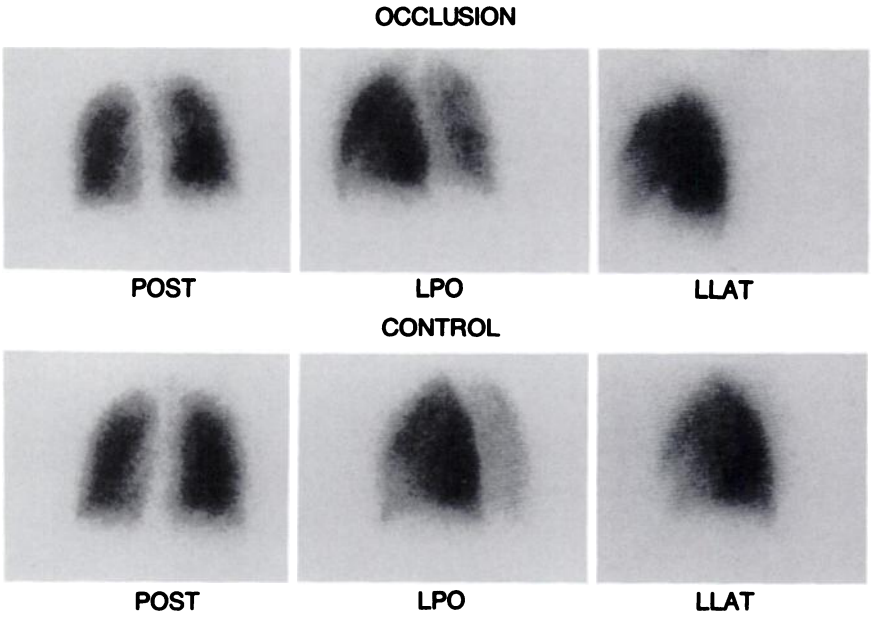

FIGURE 4. Defect involving the anterior segment of the left lower lobe. Same layout as for Figure 2. The defect is only clearly visible in the left lateral view.

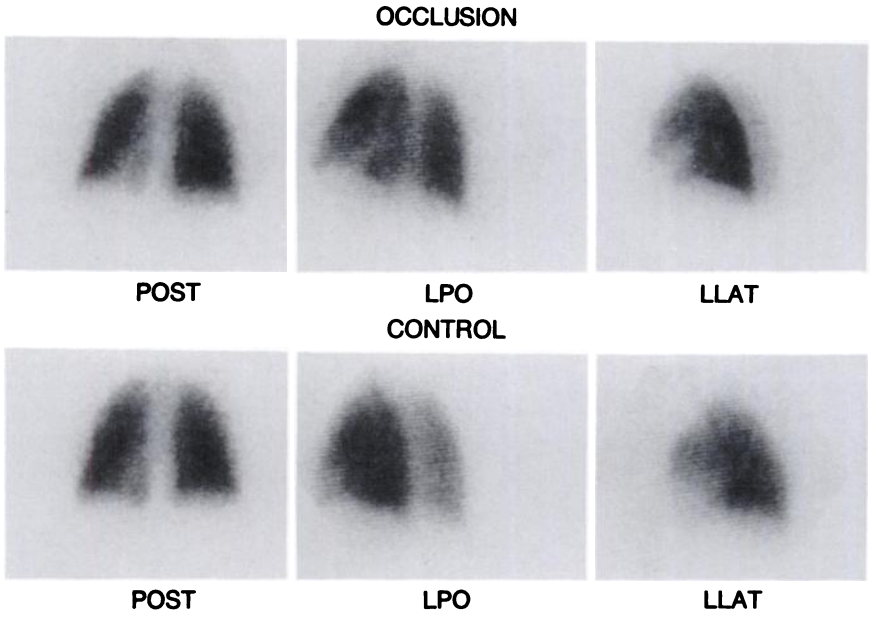

FIGURE 5. Defect involving the lateral segment of the left lower lobe. Same layout as for Figure 2. The defect is most clearly seen in the posterior-oblique view.

projection there is less overlying radioactivity from contiguous segments in the same lung. The posterior-oblique view best visualizes the more posteriorly placed segments for the same reason.

Mandell (*12*), in a study using ^{57}Co-containing lung phantoms, states that a segment should be viewed along the axis of its segmental boundaries in horizontal cross section to clearly delineate it from its neighboring segments and that the oblique views tend to sharpen the borders of segmental defects for this reason. The present study supports the first contention but not the second. The more posteriorly placed segments, especially in the lower lobes, tend to project outwards and backwards with their apices at the hilum (*22*) and it is these segments that were better visualized in the posterior-oblique view in the present study (Figs. 5 and 6). The anterior segments of both lower lobes lie just in front of the hilum (*22*) and are optimally visualized in the lateral view (Fig. 4). The other anteriorly placed segments tend to be wedge-shaped, with a large anterior pleural base and edges that are orthogonal to the lateral projection, and are therefore also better visualized in this view (Fig. 3). If the segments are considered as groups lying anterior and posterior to the hilum of the lung, these differences become even more obvious. Of the 10 segments lying predominantly anterior to the lung hilum, 9 of 10 are optimally demonstrated in the lateral view (the single segment not detected is the medial basal segment of the right lower lobe); all segments posterior to

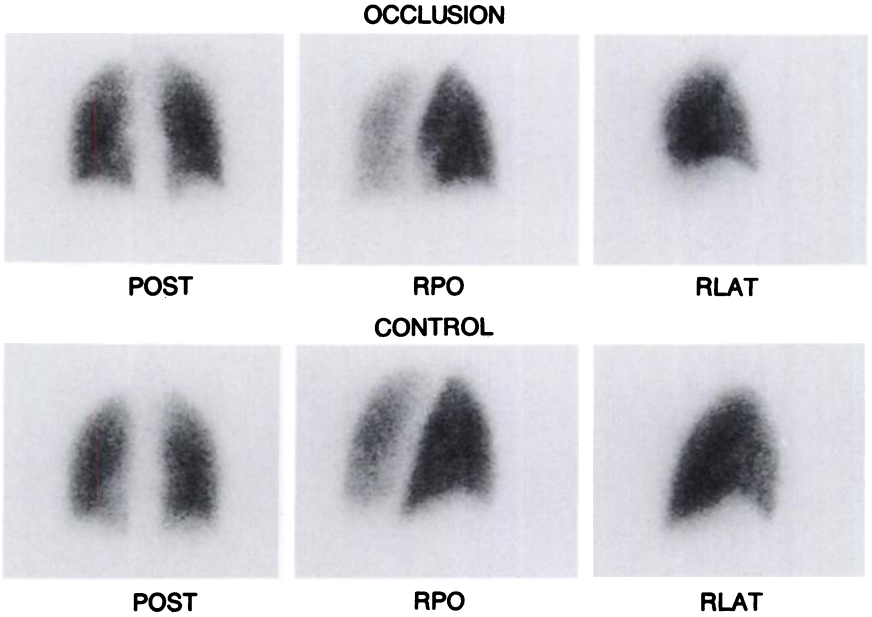

FIGURE 6. Right lower lobe posterior basal segment occlusion. Same layout as for Figure 2. Very little is seen in the posterior view. The defect is optimally demonstrated in the posterior-oblique view. (RPO = right posterior-oblique and RLAT = right lateral).

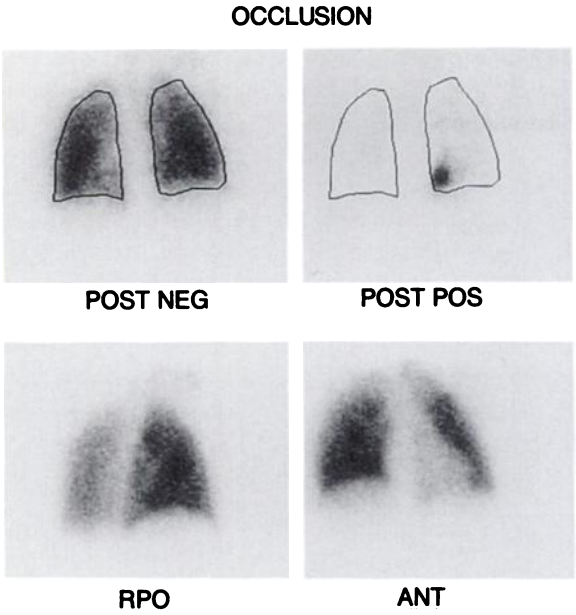

FIGURE 7. A defect involving the medial basal segment of the right lower lobe is undetectable in these views, despite its presence being demonstrated by a positive image. The positive image is seen in the posterior view and a lung outline has been added to demonstrate its position. (POST = posterior, RPO = right posterior-oblique, POS = positive image and ANT = anterior).

the hilum are better demonstrated in the posterior-oblique view.

Anterior views were performed if the defect could not be adequately visualized in the other projections. This was only necessary in the case of the medial segment of the right middle lobe and the medial segment of the right lower lobe. The anterior view might be expected to add to the detection of a defect in the medial segment of the middle lobe because the medial segment occupies virtually all of the front of the anterior surface of this lobe (*23*). However, the anterior view demonstrated only a vague attenuation of activity medially and did little to characterize the defect. The medial segment of the right lower lobe

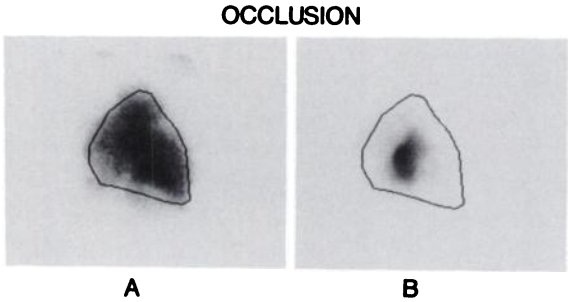

FIGURE 8. Defect involving the anterior basal segment of the left lower lobe in the left lateral view. (A) Negative image and (B) positive image of this defect. The lung outline from (A) has been superimposed on (B) to show the position of the positive image.

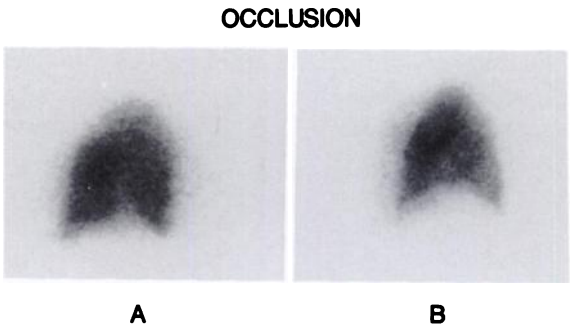

FIGURE 9. Right lateral views of a defect involving the anterior segment of the right lower lobe. (A) Subject is seated and (B) subject is supine.

remained invisible in the anterior view (Fig. 7), despite its presence being detected with a positive scan.

Table 1 also addresses the question of the minimum number of views that should be performed to miss the smallest number of potential defects; in other words, the most clinically useful views. Our data suggest that the posterior view is the least useful and that the most efficient studies in terms of defect detection and scanning time would be limited to both laterals and right and left posterior-obliques. The limited usefulness of the posterior view in detecting many defects implies that ventilation scanning methods using the posterior view alone are unreliable. However, it should be emphasized that while this is true for the detection of segmental defects, the posterior view may help to characterize other pathologies such as pleural effusion.

Direct comparison of positive and negative images confirmed the impression that many negative images, especially those involving the anterior and lateral basal segments of both lower lobes, look smaller than expected from standard texts (*24*), or when compared to their positive images (Fig. 8). This is not due to the supine position of the subjects since comparisons in the upright position showed little difference in the size of the defect (Fig. 9). The explanation may be that radioactivity in surrounding segments encroaches upon the edges of the defect, especially in the lower lobes where there is considerable overlap of the tightly packed basal segments. The best view in which to visualize a segment therefore will be the view that minimizes the degree of overlap (Fig. 10). These effects, together with imperfect collimation, could lead to a segmental defect being misinterpreted as subsegmental.

A possible criticism of our method is that collateral ventilation is occurring distal to the balloon obstruction, carrying isotope into the occluded segment and making the defect appear smaller. This is unlikely, since defects that could be easily visualized in a particular view had well-defined borders. Also, the positive images of individual segments were sharp and showed no overspill (Fig. 8). Furthermore, experimental evidence suggests that collat-

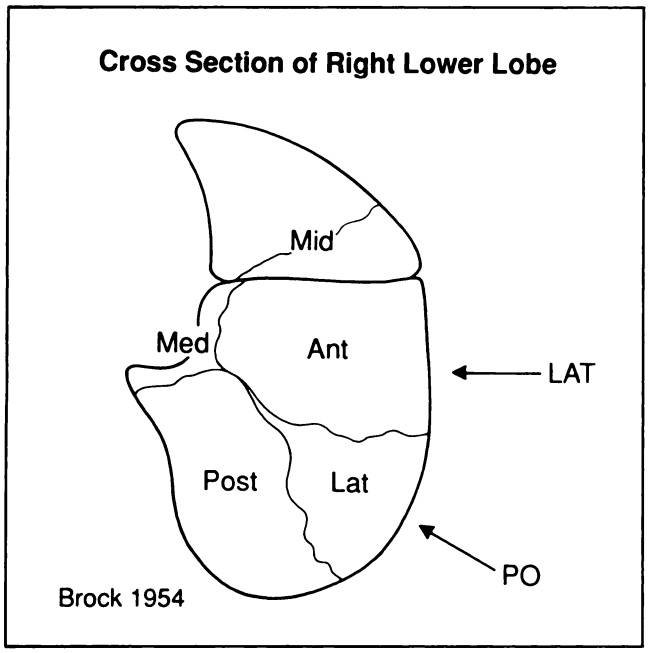

FIGURE 10. Cross section of the right lower and middle (Mid) lobes. The arrows indicate the direction of viewing (LAT = lateral and PO = posterior-oblique). It can be seen that the lateral view will best visualize the anterior basal segment (Ant) because it minimizes the degree of overlap from neighboring segmental borders. The posterior-oblique view best visualizes the posterior (Post) and lateral (Lat) basal segments for the same reason. (Med = medial basal segment). Adapted from Brock (*23*).

eral ventilation does not play a significant role in healthy humans (*25*).

Person-to-person variation exists in the anatomical distribution of individual lung segments (*23*). This variation is greater for some segments than others. For example, the anterior basal segment of the right lower lobe has a very constant distribution, whereas the corresponding segment on the left has one of the most variable (*26*). In the present study, we included only those segments with a classical distribution (*23*) on the basis of the bronchial branching pattern seen at bronchoscopy and the appearance of the positive images.

We found that defects involving the medial segment of the right middle lobe and the medial basal segment of the right lower lobe (Fig. 7) were barely detectable on a negative image. Small numbers of false-negative scans have been reported in recent prospective studies (*7,8*). Unfortunately, the sites of emboli in the false-negative scans were not identified. One recent case report, however, documents a patient with a normal ventilation-perfusion scan who was subsequently found to have an embolus completely occluding the medial basal segment of the right lower lobe at angiography (*26*).

In light of these results, we offer a reappraisal of the current concept of the segmental defect on a ventilation-perfusion lung scan. We have shown that segmental defects, especially in the anterior and lateral basal segments of the lower lobes, are often considerably smaller than line drawings in standard anatomical texts. Thus, the size of a basal segmental defect on the lung scan is not an accurate indication of its segmental or subsegmental nature: site and a triangular or hemispherical shape are more reliable criteria. Segmental defects situated anterior to the hilum of the lung are better visualized in the lateral projection and those posterior to the hilum are better visualized in the posterior-oblique projection. If these two views are performed, virtually all segmental defects will be optimally demonstrated. Segmental defects may be present at certain sites despite a virtually normal lung scan. Finally, we consider that scanning for pulmonary embolism with ventilation scans performed in the posterior view alone will be highly unreliable in the detection of segmental defects.

ACKNOWLEDGMENT

This work was supported by a North West Thames Regional Health Authority grant.

REFERENCES

1. Poulose KP, Reba RC, Gilday DL, DeLand FH, Wagner HN. Diagnosis of pulmonary embolism. A correlative study of the clinical, scan, and angiographic findings. *Br Med J* 1970;3:67–71.
2. Gilday DL, Poulose KP, DeLand FH. Accuracy of detection of pulmonary embolism by lung scanning correlated with pulmonary angiography. *Am J Roentgenol* 1972;115:732–738.
3. McNeil BJ, Holman BL, Adelstein SJ. The scintigraphic definition of pulmonary embolism. *JAMA* 1974;227:753–757.
4. Biello DR, Mattar AG, McKnight RC, Siegel BA. Ventilation-perfusion studies in suspected pulmonary embolism. *Am J Roentgenol* 1979;133: 1033–1037.
5. McNeil BJ. Ventilation-perfusion studies and the diagnosis of pulmonary embolism: concise communication. *J Nucl Med* 1980;21:319–23.
6. Cheely R, McCartney WH, Perry JR, et al. The role of noninvasive tests versus pulmonary angiography in the diagnosis of pulmonary embolism. *Am J Med* 1981;70:17–22.
7. Hull RD, Hirsh J, Carter CJ, et al. Diagnostic value of ventilation-perfusion lung scanning in patients with suspected pulmonary embolism. *Chest* 1985; 88:819–828.
8. PIOPED Investigators. Value of the ventilation/perfusion scan in acute pulmonary embolism. *JAMA* 1990;263:2753–2759.
9. Poulose K, Reba RC, Wagner HN. Characterization of the shape and location of perfusion defects in certain pulmonary diseases. *N Engl J Med* 1968;279:1020–1025.
10. Neumann RD, Sostman HD, Gottschalk A. Current status of ventilation-perfusion imaging. *Semin Nucl Med* 1980;10:198–217.
11. Carbonell AM, Landis GA, Miale A, Moser KM. Construction and testing of a thorax-lung phantom to aid in scintiphotograph interpretation. *Invest Radiol* 1969;4:275–285.
12. Mandell CH. *Scintillation camera lung imaging: an anatomic atlas and guide.* London: Grune and Stratton; 1976.
13. Fogelman I, Maisey M. Lung. In: *An atlas of clinical nuclear medicine.* London: Martin Dunitz; 1988:596–640.
14. Myers J. The practical estimation of internal radiation doses from ^{81m}Kr and similar ultra-short lived radionuclides. *Nucl Med Comm* 1981;2: 358–364.
15. Fazio F, Jones T. Assessment of regional ventilation by continuous inhalation of radioactive krypton-81m. *Br Med J* 1975;3:673–676.
16. Appleton AB. Segments and blood-vessels of the lungs. *Lancet* 1944;ii: 592–594.
17. Nielsen PE, Kirchner PT, Gerber FH. Oblique views in lung perfusion scanning: clinical utility and limitations. *J Nucl Med* 1977;18:967–973.
18. Caride VJ, Puri S, Slavin JD, et al. The usefulness of the posterior oblique views in perfusion lung imaging. *Radiology* 1976;121:669–671.
19. Moser KM, Harsanyi P, Rius-Garriga C, Guisan M, Landis GA, Miale A. Assessment of pulmonary photoscanning and angiography in experimental

pulmonary embolism. *Circulation* 1969;39:663–674.
20. Wellman HN, Mack JF, Saenger EL, Friedman BI. Clinical experience with oblique views in pulmonary perfusion scintigraphy in normal and pathological anatomy. *J Nucl Med* 1968;9:374.
21. Surprenant EL, Browning N, Webber MM. The significance of shine-through on the side view lung scan. *J Nucl Med* 1967;8:400.
22. Foster-Carter AF. The anatomy of the bronchial tree. *Br J Tuberculosis* 1942;36:19–39.
23. Brock RC. *The anatomy of the bronchial tree*, 2nd edition. London: Oxford University Press; 1954.
24. Anderson JE. *Grant's atlas of anatomy*, 7th edition. London: Williams and Wilkins; 1980.
25. Terry PB, Traystman RJ, Newball HH, et al. Collateral ventilation in man. *N Engl J Med* 1978;298:10–15.
26. Berg RM, Boyden EA, Smith FR. An analysis of the segmental bronchi of the left lower lobe of fifty dissected, and ten injected, lungs. *J Thorac Surg* 1949;18:216–236.
27. Ceraldi CM, Schabel SI, Waxman K. Normal ventilation/perfusion lung scan in a patient with proven pulmonary embolus. *Crit Care Med* 1990; 18:577–578.

(continued from page 642)

SELF-STUDY TEST

4. This 66-yr-old man with known chronic lymphocytic leukemia has pain in his left thigh and low-grade fever. You are shown an anterior image from a ^{99m}Tc MDP bone scan (Fig. 2) and anterior and left lateral images obtained with ^{67}Ga citrate (Fig. 3.) Which *one* of the following is the best explanation for the focal abnormality (arrow) in the left femur?

A. Acute osteomyelitis
B. Acute infarct
C. Chronic infarct
D. Leukemic infiltration
E. Metastatic carcinoma

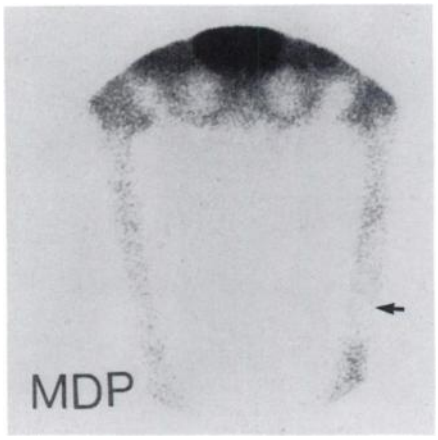

R Ant L

Figure 2

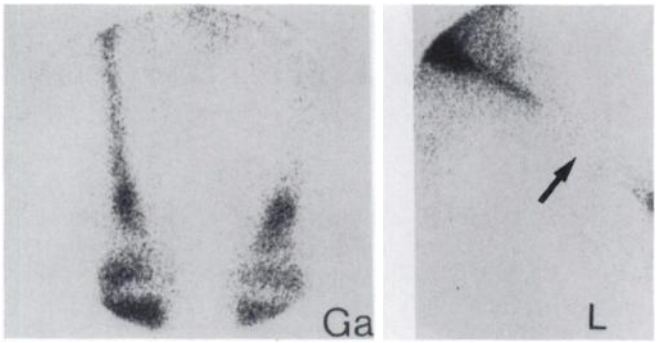

R Ant L Lat

Figure 3

5. This 58-yr-old woman has had pain and swelling of the right hand for several weeks. You are shown images from three-phase skeletal scintigraphy with ^{99m}Tc MDP (Fig. 4). Which *one* of the following is the most likely diagnosis?

A. Rheumatoid arthritis
B. Calcium pyrophosphate dihydrate (CPPD) crystal deposition disease
C. Reflex sympathetic dystrophy syndrome
D. Cellulitis
E. Post-traumatic arteriovenous fistula

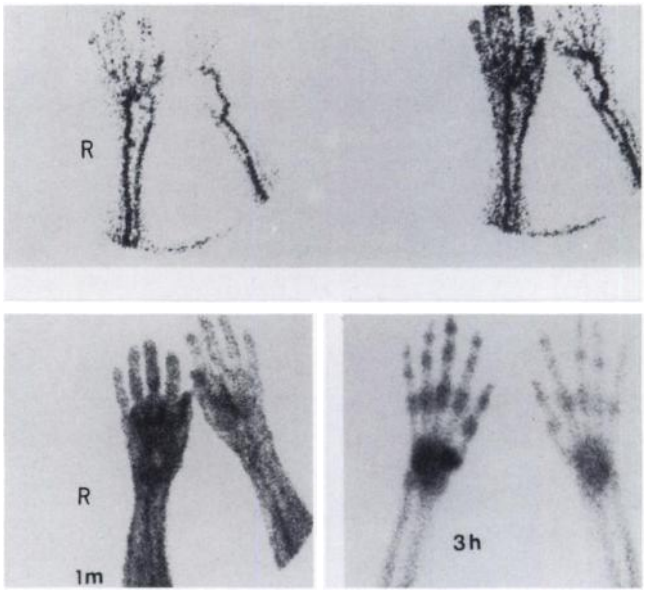

Figure 4

6. Which *one* of the following is the *least* likely scintigraphic finding expected with a 1-wk-old, uncomplicated fracture?

A. Increased perfusion at the fracture site on radionuclide angiography with ^{99m}Tc MDP.
B. Increased "blood-pool" activity at the fracture site on an immediate image with ^{99m}Tc MDP.
C. Increased concentration of ^{99m}Tc MDP at the fracture site on a 3-hr delayed image.
D. Increased uptake of ^{67}Ga citrate at the fracture site.
E. Increased uptake of ^{111}In-labeled leukocytes at the fracture site.

(continued on page 747)